International Research Journal of Engineering and Technology (IRJET) e-ISSN: 2395-0056
Volume: 11 Issue: 03 | Mar 2024 www.irjet.net p-ISSN: 2395-0072

Comparative Analysis of Heat Transfer and Skin Friction Characteristics in Circular and Diamond Shaped Tube Bank Arrangements

MD. Rashid Hussain[1], Dr. Ajay Singh[2], Ashish Verma[3]

[1]*Scholar, Department of Mechanical Engineering, Radharaman Institute of Technology and Science, Bhopal, M.P, INDIA*
[2]*Head and Prof., Department of Mechanical Engineering, Radharaman Institute of Technology and Science, Bhopal, M.P, INDIA*
[3]*Assistant Professor, Department of Mechanical Engineering, Radharaman Institute of Technology and Science, Bhopal, M.P, INDIA*

Abstract - *This research paper investigates the heat transfer and skin friction characteristics of tube bank arrangements, comparing circular and diamond-shaped configurations. The study explores how variations in longitudinal pitch impact Nusselt number and skin friction coefficient for different Reynolds numbers. The findings reveal several significant conclusions. First, transitioning from a circular tube arrangement to a diamond-shaped triangular tube bank arrangement results in a remarkable 35% reduction in skin friction coefficient. This substantial decrease underscores the potential benefits of diamond-shaped tube banks in terms of reducing drag and energy consumption. Second, the research indicates that for circular tube banks, the Nusselt number reaches its peak value when the longitudinal pitch is 2.5 times the tube diameter (2.5D). This optimal pitch length holds true across various Reynolds numbers, demonstrating the consistency of heat transfer performance in circular tube bank arrangements. Similarly, the skin friction coefficient in circular tube banks also reaches its maximum value at a longitudinal pitch of 2.5D, aligning with the Nusselt number trend. In contrast, the study highlights specific nuances in diamond-shaped tube bank arrangements. Initially, the Nusselt number is maximized at a longitudinal pitch of 2D for Reynolds numbers up to 12,000. However, beyond this threshold, a longitudinal pitch of 3D offers the highest Nusselt number values, indicating a transition in optimal pitch length. Additionally, in diamond-shaped tube banks, the minimum skin friction coefficient is achieved with a longitudinal pitch of 2.5D, showcasing a distinct behavior compared to circular arrangements. This research paper provides valuable insights into the performance differences between circular and diamond-shaped tube bank arrangements, shedding light on the potential for optimizing heat transfer and reducing drag in various engineering applications.*

Key Words: Tube Bank Arrangement, CFD, Diamond Shape, Circular Shape, Skin Friction Coefficient, Nusselt Number

1.INTRODUCTION

Tube bank arrangements play a pivotal role in numerous engineering and industrial applications where heat transfer, pressure drop, and energy efficiency are critical concerns. These configurations of closely packed tubes are extensively used in heat exchangers, boilers, condensers, and other systems to facilitate the exchange of thermal energy between a fluid and solid surface. The efficiency and performance of these systems are significantly influenced by the geometric arrangement of the tubes within the banks. The design of tube banks involves a delicate balance between maximizing heat transfer rates and minimizing the associated pressure drop or skin friction. Achieving this balance is of paramount importance in enhancing the overall effectiveness of heat exchangers and similar devices. Engineers and researchers have, therefore, devoted considerable efforts to understanding the impact of various tube bank configurations on heat transfer and fluid flow characteristics. One intriguing area of investigation is the comparison between traditional circular tube arrangements and alternative geometric configurations, such as diamond-shaped triangular tube banks. By altering the shape and orientation of tubes within a bank, it is possible to significantly influence heat transfer and fluid dynamics, potentially leading to more efficient and cost-effective solutions. This research aims to contribute to this ongoing discourse by systematically analysing and comparing the performance of circular and diamond-shaped tube bank arrangements. This paper presents a comprehensive examination of the Nusselt number, a dimensionless parameter used to quantify heat transfer, and the skin friction coefficient, a measure of drag, for both circular and diamond-shaped tube banks. We investigate how variations in longitudinal pitch impact these parameters across different Reynolds numbers, shedding light on the optimal configurations for various engineering applications. The findings of this research are expected to have far-reaching implications, offering valuable insights into the design and optimization of tube bank arrangements to meet the demands of diverse industries, from aerospace to energy production, where heat exchange and fluid flow are fundamental processes.

2. LITERATURE REVIEW

Mustafa Erguvan et al. [1], The paper investigates energy and exergy analyses of unsteady cross-flow over heated circular cylinders through numerical simulations, considering various parameters such as the number of inline tubes, inlet velocity, pitch ratios, and Reynolds number. The energy efficiency ranges from 72% to 98% for all cases, with viscous dissipation having a minimal effect on energy efficiency at low Reynolds numbers. **Waheed Ahmad et al. [2],** This study investigates the ideal spacing between diamond-shaped cooling tubes using free convection. Diamond-shaped tubes are arranged in a fixed space, and the spacing is determined by Bejan's constructal theory, maximizing heat transfer density. **Yi Chun Li et al. [3],** The paper explores the impact of wake region on thermohydraulic performance in finned tube heat exchangers using section-streamlined tubes. Numerical simulations validate the proposed tube configurations and angle θ, showing improved overall performance compared to traditional tube shapes. S**. Sahamifar et al. [4],** The paper presents a numerical optimization study using a generalized pattern search algorithm to find the optimum longitudinal and transverse pitches of cross-flow staggered tube banks in turbulent flow regime. The study shows that the optimum dimensionless longitudinal and transverse pitches of the staggered tube banks are independent of the inlet Reynolds and Prandtl numbers in the turbulent regime and equal to PL, opt ≅ 1 and PT, opt ≅ 1.3, respectively. **Nasif Kuru et al. [5],** The paper investigates the numerical optimization of heat and fluid flow over staggered tube banks, both with and without axial fins. Ansys Fluent software is used for the numerical computation. **Tahir Erdnic et al. [6],** The study investigates the thermo-hydraulic characteristics of circular and diamond-shaped cross-sections in periodic flow using numerical simulations. The main objective is to determine if diamond-shaped cross-sections can provide better thermal performance compared to circular ones.. **Tahir Erdnic et al. [7],** The paper focuses on the computational thermal-hydraulic analysis and geometric optimization of circular and elliptic wavy fin and tube heat exchangers (FTHE) in a staggered arrangement. The analysis is conducted using numerical optimization studies with mode FRONTIER 2021R3 software and computational fluid dynamics (CFD) analysis with ANSYS Fluent R2021a.. **A Alamir et al. [8],** The paper proposes an artificial neural network (ANN) model for predicting the cooling temperature and performance of a thermoacoustic refrigerator (TAR). Two ANN models were presented with different numbers of neurons in the hidden layers, and the results showed high accuracy in predicting TAR cooling temperature and performance. The use of two hidden layers was found to be sufficient for achieving the highest model accuracy. **Fatimah Al Zahra et al. [9],** Thermoacoustic involves the conversion of thermal and acoustical energies for green technology applications. This paper focuses on the oscillatory flow within a parallel-plate structure in a standing-wave thermoacoustic system, studying the effects of the entrance and exit regions on the flow dynamics.. **J. Yaio et al. [10],** This paper introduces a methodology for modeling occupants' stochastic behavior with regard to air conditioning in buildings. This approach combines measured data, statistical analysis, and logistic regression to create models that predict when occupants are likely to turn on the air conditioning, at what temperature they will set it, and when they will turn it off. **Iikar Gokay et al. [11],** Thermoacoustic cooling systems are not well compared to compressor compression cooling systems, and this study aims to investigate and solve the reasons for this. The performance of a thermoacoustic cooling system depends on various factors, and this study focuses on the effect of different waveforms on heat transfer in a thermoacoustic cooler. **S Gabriel et al. [12],** Pulsatile blood flow induces local flow disturbances characterized by significant oscillations, which have physiological significance in the cardiovascular system, particularly in relation to their proatherogenic expression on endothelial cells. **Anas A Rehman et al. [13],** The paper presents the application of artificial neural network (ANN) technique to predict the oscillatory heat transfer coefficient in thermoacoustic heat exchangers under different operating conditions. The ANN model developed for a standing wave thermoacoustic refrigerator shows promising accuracy in predicting the oscillatory heat transfer coefficient compared to experimental and calculated results from other correlations in the literature. **Alberto Alberellio et al. [14],** The paper investigates the existence and properties of non-breaking, wave-induced turbulent flow in the ocean, which injects mixing into subsurface layers. The authors present measurements of the velocity field of oscillatory flows induced by mechanically generated random wave fields, demonstrating a power-law scaling in the spectral tail of the velocity field and highlighting the emergence of intermittency in oscillatory flows through statistical analysis of structure functions. **Mario R et al. [15],** The study investigates the impact of different surface roughness values on copper tubes in pool boiling of water, finding that even small increments in surface roughness, along with the addition of hydrophobic patterns, can significantly enhance heat transfer. **Chidanand K et al. [16],** The paper investigates the use of longitudinal splitter plates as fins in a staggered cross flow tube bank for heat transfer enhancement. The geometric configuration of the splitter plates, such as length and thickness, is varied to improve the overall thermal-hydraulic performance of the tube bank. Experimental and numerical studies are conducted to evaluate the effects of different splitter plate configurations on the Nusselt number and pressure drop. **A. M. N. Elmekawy et al. [17],** The paper investigates the effect of attaching a splitter plate to the circular tube on the performance of a heat exchanger with a circular tube bank, using a CFD model to simulate the cross-flow behaviour inside the heat exchanger. Results show that attaching splitter plates to the tubes can reduce pressure drop and increase the Nusselt number, leading to better overall thermal performance for the heat exchangers. **M. E. Nakhchi et al. [18],** The paper presents a numerical investigation of the turbulent characteristics and thermal enhancement parameter of CuO-water nanofluids in heat exchangers enhanced with double V-cut twisted tapes. The study explores the effects of twist ratio, cut ratio, Reynolds number, and nanoparticles volume fraction on fluid mixing and heat transfer enhancement. The results show that the modified twisted tapes with cuts improve fluid mixing and heat transfer, leading to a 14.5% increase in heat transfer for a nanofluid with a volume fraction of 1.5%. **H. A. Refaey et al. [19],** The paper presents 2-D numerical investigations of turbulent flow over a staggered tube bank using a commercial CFD package, focusing

on the effect of various parameters on heat transfer and flow characteristics. The simulation results are compared with experimental data and previous analytical results, showing acceptable agreement. **Ram P. Bharti et al. [20],** The paper investigates the steady flow of non-Newtonian power-law fluids through a periodic square array of circular cylinders using numerical simulations. The study explores the flow characteristics by varying the fluid volume fraction, Reynolds number, and power-law index. The steady flow of non-Newtonian power-law fluids across a periodic square array of infinitely long circular cylinders is studied numerically using an unstructured finite volume method.

3. METHODOLOGY

This project focuses on analyzing circular and diamond-shaped tubes arranged in a triangular pattern to enhance thermal performance through passive methods without increasing project costs. The study was conducted using ANSYS 2022R1. The impact of the diamond shape in a triangular tube bank arrangement on the Nusselt number and skin friction coefficient is examined. Skin friction coefficient and Nusselt number variations with Reynolds number under specific parameters are determined. Diamond-shaped tubes are found to induce better turbulent flow compared to circular tubes due to a large pressure gradient at the tube's tail end. After reaching the minimum pressure value, an inverse pressure gradient forms, leading to the formation of vortices, intensifying turbulence and enhancing thermal performance. The inline tube bank arrangement features an inlet at 3D from the first column and an exit at 20D from the last column, with constant longitudinal and transverse pitch values of 3D.

The literature survey suggests that SST and turbulence K-epsilon models are suitable for tube bank arrangements in cross-flow heat exchangers. After simulating both models, the K-epsilon model produces more accurate results. The selection of the turbulence model is crucial, given differing recommendations from various authors, and no prior research on CFD analysis of triangular tube bank arrangements. SST-K-epsilon was found to be the most suitable model for simulating the inline tube bank arrangement, as explained in the following steps.

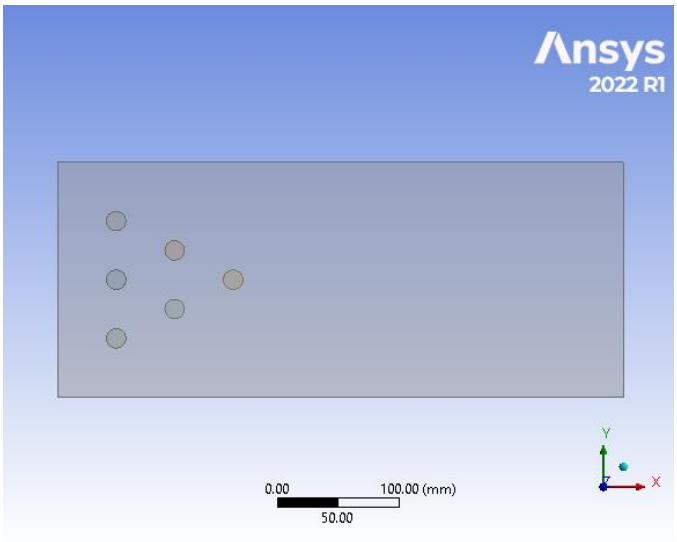

Figure 1: Circular Shape Triangular Tube Bank Arrangement

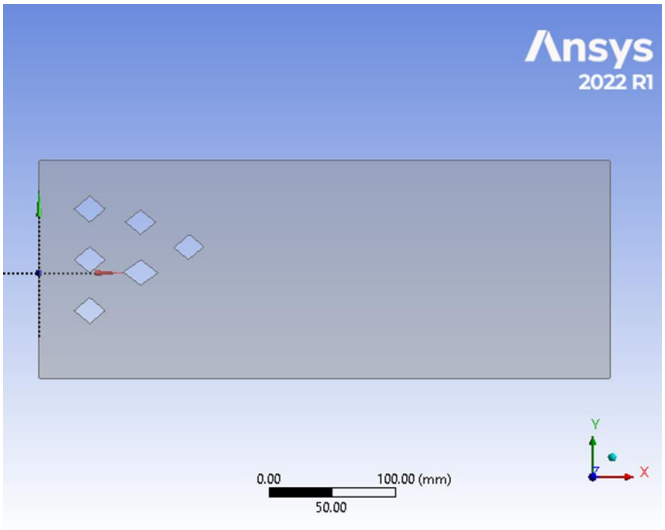

Figure 2: Diamond Shape Triangular Tube Bank Arrangement

3.1. Assumptions

Numerical model was developed under the following assumptions

1. The physical properties of the working fluid and the tube are constant.
2. The incompressible flow is limited as laminar flow.
3. The flow and heat transfer are in steady state.
4. The viscous dissipation is negligible.

3.2. Boundary Conditions

The first case involves circular-shaped tubes arranged in a compact triangular pattern. This arrangement requires less space compared to inline and staggered grid layouts. Inlet and outlet sections are positioned at specific distances from the tubes, measured from the tube center, to ensure uniform velocity distribution at the inlet and fully developed flow at the outlet. Boundary conditions are applied as follows:

1. At the entrance velocity is given with 3, 4, 6, 8, 10 m/s.
2. The tube is given wall as no slip condition with the heat generation of 25000 W.
3. Top and bottom walls are adiabatic with pressure outlet conditions.

The null value of pressure is applied at all the boundary conditions.

3.3. Mesh Generation

Structured mesh is generated over the tube bank arrangement and the domain, and first cell height of the mesh (dy) near to the wall of the tube is 0.0000026 according to the value of Y+ equal to one. The value of Y+ indicates the distance up to which boundary layer will be pronounced and it governs the production of kinetic energy. Mesh details are as fallow, Y+ equal to one, a total number of nodes equal to 71517 and quality of the mesh will be more than 80%. After mesh generation the mesh is solved numerically with CFD solution. Fig.2.3 shows schematic drawing of the present computational domain. The structured mesh of element size 71517 is developed with near wall mesh refinement of Y+=1.0 and the mesh quality is above 90%.

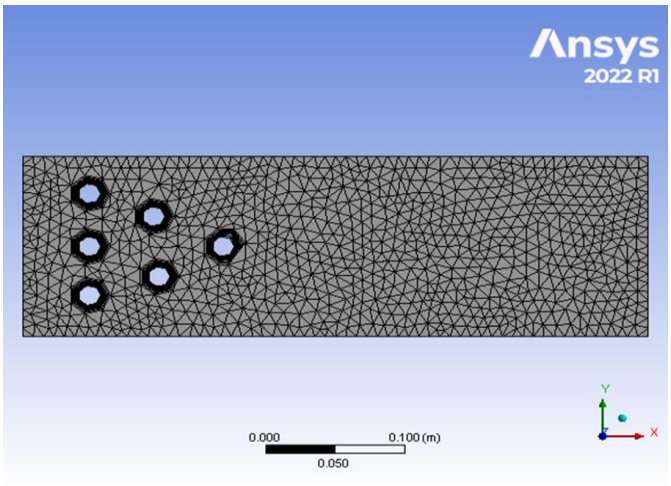

Figure 3: Meshed Geometry

In this study, air as the working fluid flows through a domain with velocities ranging from 2 m/s to 10 m/s, corresponding to Reynolds numbers of 6477 to 18127. A pressure-based solver with the SST-K epsilon model and first-order upwind flow is employed. The diamond-shaped tube surface has a no-slip boundary, while domain boundaries have slip conditions. The outlet is set as a pressure outlet at atmospheric pressure, and the diamond-shaped tubes generate 25000W of heat. The simulation, conducted in 2D, examines the impact of Reynolds number on a triangular tube bank arrangement, involving geometry, modelling, mesh generation, CFD solution, and analysis of results.

4. RESULTS AND DISCUSSION

The SST k-€ turbulence model proves superior for external flow over a circular-shaped triangular tube bank. The study explores different solvers with this model for analysis and discusses the results. Simulation is done at pressure-based solver and the scheme is SIMPLE and boundary condition for given geometry of tube is defined in table 1. Solution initialization is standard with the absolute reference frame.

Table 1: Parameter and Input Values

Parameters	Input Values
Analysis Type	Pressure Based, Steady State, Scheme-SIMPLE
Turbulence Model	k-€ (SST)
Material Fluid	Water (Density Constant)
Inlet	Velocity Inlet
Circular Tube Surface	No Slip
Domain Boundaries	
Top	Pressure Outlet
Bottom	Pressure Outlet
Inlet	Wall (No Shear)
Outlet	Wall (No Shear)

4.1. For Circular Shaped Tubes

From table 2 to table 4, different values of Nusselt Number and Skin Friction Coefficient for circular shaped tubes are mentioned and the reading were taken from ANSYS 2022R1.

Table 2: Data for Nusselt Number and Skin Friction Coefficient wrt Reynolds Number for Pitch of 3D

Reynolds Number	Nusselt Number	Skin Friction Coefficient
6477	60.09	0.023
9729	67.7	0.017
12972	77.3	0.016
16215	87.46	0.015
18127	92.65	0.013

The table 2 Nusselt number increases with rising Reynolds number, evident from Fluent data. This relationship approximates a straight line, aligning with theoretical expectations of Nusselt number growth with increasing Reynolds number. The highest Nusselt number, 92.65, occurs at Reynolds number 18127 with a longitudinal pitch of 3D. In contrast, the skin friction coefficient decreases with higher Reynolds numbers, exhibiting a steep initial decline from 0.022184 to 0.016938, followed by a gradual decrease to 0.014127. This aligns with the inverse relationship between skin friction coefficient and Reynolds number in fluid mechanics.

Table 3: Data for Nusselt Number and Skin Friction Coefficient wrt Reynolds Number for Pitch of 2.5D

Reynolds Number	Nusselt Number	Skin Friction Coefficient
6477	69.93	0.0285
9729	78.8	0.0217
12972	86.78	0.019
16215	97.85	0.0185
18127	103.49	0.018

The table 3 shows Nusselt number increasing with Reynolds number, as observed in Fluent data. When compared to a longitudinal pitch of 3D, there's a slight increment. The highest Nusselt number, 103.49, occurs at Reynolds number 18127 with a horizontal pitch of 2.5D. The graph also reveals a steep decline in skin friction coefficient from 0.028463 to 0.021723, followed by a gradual decrease to 0.018023 with increasing Reynolds number, aligning with the expected trend of decreasing skin friction with higher Reynolds numbers.

Table 4: Data for Nusselt Number and Skin Friction Coefficient wrt Reynolds Number for Pitch of 2D

Reynolds Number	Nusselt Number	Skin Friction Coefficient
6477	70.6	0.027959
9729	79.81	0.022515
12972	86.98	0.019684
16215	97.35	0.018761
18127	102.61	0.01826

The table 4 illustrates the relationship between skin friction coefficient and Reynolds number for a longitudinal pitch of 2D. The highest skin friction coefficient (0.0279588) occurs at Reynolds number 6477, followed by a steep decline to 0.022515 and gradual decreases at higher Reynolds numbers.

4.2. For Diamond Shaped Tubes

From table 5 to table 7, different values of Nusselt Number and Skin Friction Coefficient for diamond shaped tubes are mentioned and the reading were taken from ANSYS 2022R1.

Table 5: Data for Nusselt Number and Skin Friction Coefficient wrt Reynolds Number for Pitch of 3D

Reynolds Number	Nusselt Number	Skin Friction Coefficient
6477	61.54	0.018291
9729	77.62	0.014678
12972	93.19	0.013254
16215	107.92	0.012082

The table 5 demonstrates that Nusselt number increases with higher Reynolds numbers, aligning with Fluent data. This relationship forms a straight line, consistent with the theoretical expectation of Nusselt number growth with increased Reynolds number. The highest Nusselt number, 107.92, occurs at a Reynolds number of 18127. In contrast, skin friction coefficient decreases with rising Reynolds numbers, showing an initial steep decline followed by a gradual decrease in line with the established trend.

Table 6: Data for Nusselt Number and Skin Friction Coefficient wrt Reynolds Number for Pitch of 2.5D

Reynolds Number	Nusselt Number	Skin Friction Coefficient
6477	62.24	0.017633
9729	75.39	0.013874
12972	87.16	0.011616
16215	97.96	0.010269

The table 6 illustrates Nusselt number increasing with higher Reynolds numbers, confirmed by Fluent data. Simultaneously, the graph displays a decrease in skin friction coefficient with rising Reynolds numbers, characterized by an initial steep decline followed by a gradual reduction.

Table 7: Data for Nusselt Number and Skin Friction Coefficient wrt Reynolds Number for Pitch of 2D

Reynolds Number	Nusselt Number	Skin Friction Coefficient
6477	63.94	0.018636
9729	79.46	0.014746
12972	92.21	0.012526
16215	103.81	0.011126

The table 7 shows Nusselt number increasing with Reynolds number, consistent with Fluent data and theoretical expectations. It forms a straight-line relationship. The highest Nusselt number, similar to the value at a longitudinal pitch of 3D, is observed. Simultaneously, the graph reveals a decrease in skin friction coefficient with higher Reynolds numbers, characterized by an initial steep decline followed by a gradual reduction.

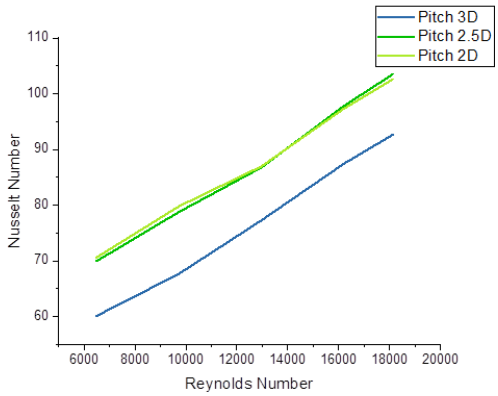

Chart 1: Comparison of Nusselt number vs. Reynolds number for circular tube

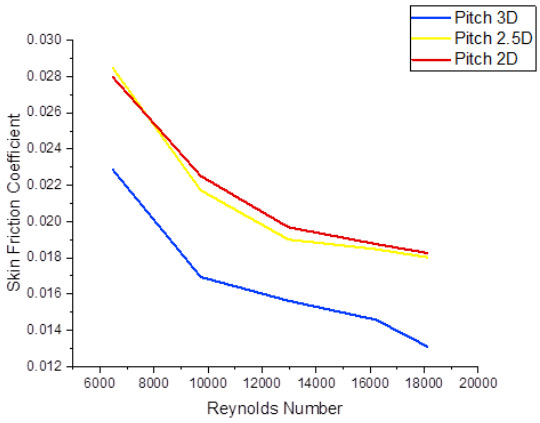

Chart 2: Comparison of Skin Friction Coefficient vs. Reynolds number for circular tube

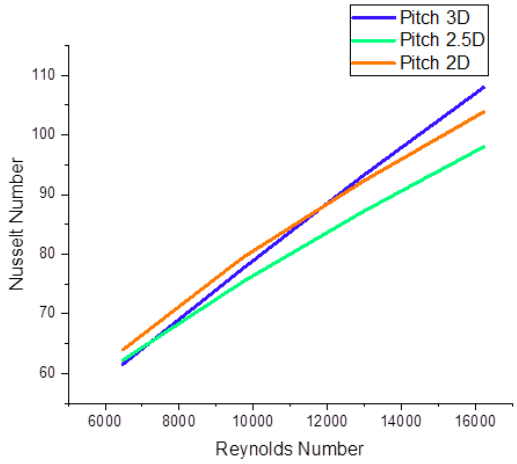

Chart 3: Comparison of Nusselt number vs. Reynolds number for Diamond Tube

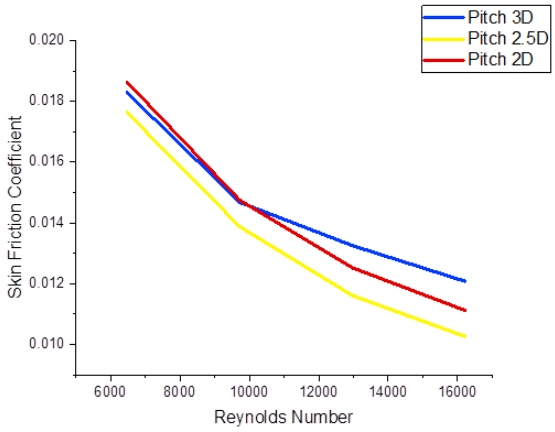

Chart 4: Comparison of Skin Friction Coefficient vs. Reynolds number for Diamond Tube

5. CONCLUSIONS

In comparing circular and diamond-shaped tube triangular tube bank arrangements, a substantial 35% reduction in skin friction coefficient is observed for the latter. For circular tubes, the Nusselt number is highest with a longitudinal pitch of 2.5D at various Reynolds numbers. Similarly, the skin friction coefficient peaks at a longitudinal pitch of 2.5D. However, for diamond-shaped tubes, Nusselt number is initially highest at 2D up to a Reynolds number of 12,000, but beyond that, 3D becomes optimal. The lowest skin friction coefficient for diamond-shaped tubes occurs with a longitudinal pitch of 2.5D.

REFERENCES

[1] M. Erguvan, D.W. MacPhee, Energy and exergy analyses of tube banks in waste heat recovery applications, Energies 11 (2018), https://doi.org/10.3390/ en11082094.

[2] A. Waheed, A. Adil, A. Razzaq, The optimal spacing between diamond-shaped tubes cooled by free convection using constructal theory, Proc. Rom. Acad. Ser. A- Mathematics Phys. Tech. Sci. Inf. Sci. 19 (2018) 129–134.

[3] Y. Li, Z. Qian, Q. Wang, Numerical investigation of thermohydraulic performance on wake region in finned tube heat exchanger with section-streamlined tube, Case Stud. Therm. Eng. 33 (2022), 101898, https://doi.org/10.1016/j. csite.2022.101898.

[4] S. Sahamifar, F. Kowsary, M.H. Mazlaghani, Generalized optimization of cross-flow staggered tube banks using a subscale model, Int. Commun. Heat Mass Tran. 105 (2019) 46–57, https://doi.org/10.1016/j.icheatmasstransfer.2019.03.004.

[5] M. Nasif Kuru, M.T. Erdinc, A. Yilmaz, Optimization of heat transfer and pressure drop in axially finned staggered tube banks, Heat Tran. Eng. 42 (2021) 1268–1285, https://doi.org/10.1080/01457632.2020.1785696.

[6] M.T. Erdinc, A.E. Aktas, M.N. Kuru, M. Bilgili, O. Aydin, An optimization study on thermo-hydraulic performance arrays of circular and diamond shaped cross- sections in periodic flow, Int. Commun. Heat Mass Tran. 129 (2021), 105706,https://doi.org/10.1016/j.icheatmasstransfer.2021.105706.

[7] M.T. Erdinc, Computational thermal-hydraulic analysis and geometric optimization of elliptic and circular wavy fin and tube heat exchangers, Int. Commun. Heat Mass Tran. 140 (2023), 106518, https://doi.org/10.1016/j. icheatmasstransfer.2022.106518.

[8] M.A. Alamir, An artificial neural network model for predicting the performance of thermoacoustic refrigerators, Int. J. Heat Mass Transf. 164 (2021) 120551.

[9] W.A. Allafi, F.A.Z.M. Saat, Entrance and exit effects on oscillatory flow within parallel-plates in standing-wave thermoacoustic system with two different operating frequencies, J. King Saud Univ.-Eng. Sci. (2020).

[10] J. Yao, Modelling and simulating occupant behaviour on air conditioning in residential buildings, Energy Build. 175 (2018) 1–10.

[11] I. G¨okay, R. Karabacak, Experimental investigation of the effect of different waveforms on heat transfer in a thermoacoustic cooler, Int. J. Refrig. (2021).

[12] S.A. Gabriel, Y. Ding, Y. Feng, Quantifying the influence of oscillatory flow disturbances on blood flow, J. Theor. Biol. 430 (2017) 195–206.

[13] A.A. Rahman, X. Zhang, Prediction of oscillatory heat transfer coefficient for a thermoacoustic heat exchanger through artificial neural network technique, Int. J. Heat Mass Transf. 124 (2018) 1088–1096.

[14] A. Alberello, M. Onorato, F. Frascoli, A. Toffoli, Observation of turbulence and intermittency in wave-induced oscillatory flows, Wave Motion 84 (2019) 81–89.

[15] M.R.M. Arenales, S. Kumar, L. Kuo, P. Chen, Surface roughness variation effects on copper tubes in pool boiling of water, Int. J. Heat Mass Tran. 151 (2020), 119399, https://doi.org/10.1016/j.ijheatmasstransfer.2020.119399.

[16] C.K. Mangrulkar, A.S. Dhoble, J.D. Abraham, S. Chamoli, Experimental and numerical investigations for effect of longitudinal splitter plate configuration for thermal-hydraulic performance of staggered tube bank, Int. J. Heat Mass Tran. 161 (2020), 120280, https://doi.org/10.1016/j. ijheatmasstransfer.2020.120280.

[17] A.M.N. Elmekawy, A.A. Ibrahim, A.M. Shahin, S. Al-Ali, G.E. Hassan, Performance enhancement for tube bank staggered configuration heat exchanger – CFD Study, Chem. Eng. Process: Process Intensif. 164 (2021), 108392, https://doi.org/10.1016/j.cep.2021.108392.

[18] M.E. Nakhchi, J.A. Esfahani, Numerical investigation of turbulent CuO–water nanofluid inside heat exchanger enhanced with double V-cut twisted tapes, J. Therm. Anal. Calorim. (2020), https://doi.org/10.1007/s10973-020-09788-4.

[19] H.A. Refaey, A.M. Sultan, M. Moawad, M.A. Abdelrahman, Numerical investigations of the convective heat transfer from turbulent flow over staggered tube bank, J. Inst. Eng. India Ser. C 100 (6) (2019) 983–993, https://doi.org/10.1007/s40032-018-0493-z.

[20] R. P. Bharti, R.P. Ram, A.K. Dhiman, Computational analysis of cross-flow of power-law fluids through a periodic square array of circular cylinders, AsiaPac. J. Chem. Eng. (2022) e2748 .